Singlet Exciplexes between a Thioxanthone Derivative and Substituted Aromatic Quenchers: Role of the Resonance Integral

Manuel Dossot, Xavier Allonas, and Patrice Jacques*[a]

Abstract: Fluorescence quenching of a thioxanthone derivative by methyl- and methoxy-substituted benzenes (MeB and MeOB, respectively) is performed in solvents of different polarity. Emissive exciplexes are observed even in polar solvents and provide kinetic and spectroscopic data over a large scale of solvent polarity. These data were subsequently analyzed by use of a new theoretical model that leads to a thermodynamic relationship between exciplex and electron-transfer driving forces ΔG_{exc} and ΔG_{et}, respectively. The remarkable agreement found between this model and both kinetic and spectroscopic data supports its validity. Moreover, the difference observed between MeB and MeOB compounds in quenching efficiency is analyzed by this model and provides the main parameters governing exciplex features, especially the resonance integral between locally excited and charge-transfer states.

Keywords: electron transfer · exciplex · fluorescence · quenching

Introduction

Charge-transfer quenching of the fluorescence of an excited acceptor molecule A* by an electron donor D in solution can follow two mechanisms:[1–4] full electron transfer[2,4,10–16] or deactivation via exciplex formation.[16–22]

1) Pure photoinduced electron transfer (PET) corresponds to the full transfer of one electron from D to A. Light excitation creates a radical ion pair $A^{\cdot-}$ $D^{\cdot+}$, with the distance between ions depending on the chemical nature of A and D and the solvation properties of the surrounding medium. The thermodynamics of PET is predicted by the free-energy change ΔG_{et} given by the Rehm–Weller equation.[1] The electronic coupling between the molecular orbitals of the two partners is low (typically <0.05 eV), and the reaction kinetics is relevant to the Marcus theory.[2,4,10–16,23–24]

2) The exciplex mechanism corresponds to the creation of a complex with only partial charge transfer between A and D and the excitation energy partly distributed over the two molecules. Such exciplexes, noted $(A^{\delta-}\ D^{\delta+})^*$ can emit fluorescence. A strong electronic coupling between the molecular orbitals of the two partners is required to stabilize the exciplex state energy. This stabilization is rationalized in the literature[5–8,17–20] by writing the exciplex wavefunction Ψ_{exc} as a linear combination of the locally excited (LE) A*D and the charge-transfer (CT) $A^{\cdot-}$ $D^{\cdot+}$ wavefunctions ([Eq. (1)].

$$\Psi_{exc} = a\Psi_{LE} + b\Psi_{CT} \quad (1)$$

The energetic stabilization is then related to the value of the resonance integral $\beta = \langle \Psi_{LE} | \mathscr{H} | \Psi_{CT} \rangle$, with $\mathscr{H}$ the Hamiltonian of the system. The involvement of Ψ_{CT} in the exciplex wavefunction implies that the free-energy change ΔG_{exc} for exciplex formation is related to ΔG_{et}. The resonance integral quantifies the relative contribution of the LE and CT states, and consequently the charge-transfer degree of the exciplex governs the fluorescence quantum efficiency.[25–31] For instance, several studies have shown exciplex luminescence in polar solvents such as acetonitrile, and these exciplexes generally had a low CT contribution.[17–18,26–33]

Herein we focus on the study of the role of the resonance integral β on exciplex properties observed in the quenching of 3-carboxyethyl-7-methyl-thioxanthen-9-one (ETX) by a set of substituted benzenes. The collected data systematically extend a preliminary observation of exciplexes in polar solvents[34,35] and are experimentally analyzed by both kinetics and spectroscopy. A new statistical thermodynamic treatment is proposed which relates ΔG_{exc} and ΔG_{et} and explicitly takes into account both the role of the resonance integral β and the effect of the medium. The very good agreement between this new model and the experimental data help to

[a] M. Dossot, X. Allonas, Prof. P. Jacques
Department of Photochemistry
Université de Haute Alsace
3, rue Alfred Werner 68093 Mulhouse Cedex (France)
Fax: (+33) 389-336-828
E-mail: p.jacques@uha.fr

 DOI: 10.1002/chem.200400269

clarify the role of β on both the kinetics and spectroscopic features of the exciplexes.

Experimental Section

All solvents were purchased from Fluka or Aldrich at the best purity grade (generally spectrophotometric grade) and used as received. Hexamethylbenzene (HMB), 1,2,4,5-tetramethylbenzene (durene), 1,3,5-trimethylbenzene (135MeB), 1,2,4-trimethylbenzene (124MeB), 1,3-dimethylbenzene (*m*-xylene), toluene, 1,2,4-trimethoxybenzene (124MeOB), 1,3,5-trimethoxybenzene (135MeOB), 1,2-dimethoxybenzene (12MeOB), 1,3-dimethoxybenzene (13MeOB), 1,4-dimethoxybenzene (14MeOB), methoxybenzene (anisole), and 4-methylanisole (4Meanisole), all from Fluka and Aldrich, were either distilled or sublimed under vacuum. Sterically hindered alkylbenzenes (HinMeB) hexaethylbenzene (HEB, Fluka), 1,1,4,4,5,5,8,8-octamethyl-1,2,3,4,5,6,7,8-octahydroanthracene (OMA, Lancaster), and 1,3,5-tritertiobutylbenzene (TTB, Aldrich) were sublimed under vacuum. 1,2,4,5-Tetramethoxybenzene (1245MeOB) was prepared according to the reference [36] and purified by recrystallization (twice) from dichloromethane. 3-Carbethoxy-7-methylthioxanthen-9-one (ETX) was a gift from Pr. E. Haselbach (Fribourg, Switzerland). Other abbreviations used in this article are as follows: MeB for methyl-substituted benzenes, MeOB for methoxy-substituted compounds, and HinMeB for encumbered alkylbenzenes.

UV/Vis absorption spectra were recorded on a Beckman DU 640 apparatus. Steady-state excitation and emission fluorescence spectra were obtained using a Fluoromax-2 spectrofluorimeter from Jobin-Yvon. No deviation occurred in excitation spectra under quencher addition. UV/Vis spectra were composed from the sum of ETX and quencher absorption bands, with no significant change that would have indicated a ground-state complex formation. Note that the concentration of electron donors was always chosen to ensure that at least 15% of singlet excited ETX were deactivated at the end of the quenching. The radius ρ of the Onsager cavity was approximated from the molecular volumes calculated by a grid method.[37,38]

The singlet state energy of ETX is $E_{0,0}=3.0$ eV, the reduction potential $E_{red}(ETX)=-1.37$ V versus SCE, and the oxidation potential of the electron donors $E_{ox}(D)$ were taken from reference [41] or measured for this work under the same conditions, the solvent being acetonitrile in all cases.

Results

Figure 1 reports the steady-state fluorescence spectra of singlet-excited ETX quenched by HMB in acetone. Addition of HMB results in a new red-shifted emission with respect to that of ETX, and simultaneously, the ETX fluorescence decreased. Since the solvatochromism of ETX fluorescence indicates that light emission would have shifted towards blue wavelengths by a reduction of polarity,[39] the red-shifted emission cannot be attributed to a local decrease of medium polarity under addition of HMB. Moreover, the dispersion effect due to a change in the refractive index was ruled out since adding cyclohexane (up to 1 M) to a solution of ETX in acetonitrile did not induce any significant change in the fluorescence spectrum. From all these experiments, the attribution of the red-shifted luminescence can be confidently assigned to the formation of an emissive exciplex between ETX and HMB.

To obtain both the exciplex emission spectrum and the quenching rate constant k_Q the usual subtraction method

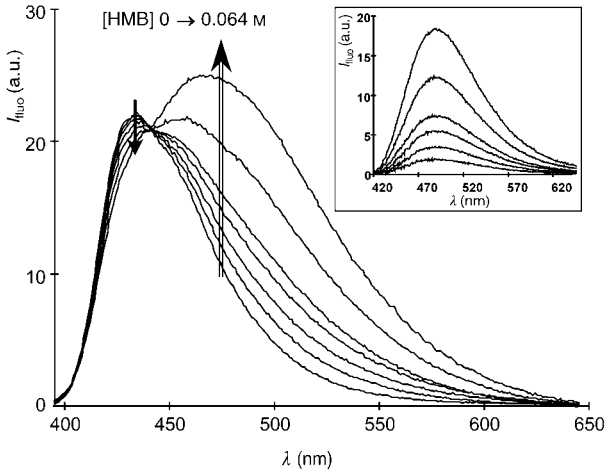

Figure 1. Fluorescence spectra obtained by addition of increasing amounts of HMB in an acetone solution of ETX. Insert : exciplex emission spectra obtained by the subtraction method.

was used, leading to a pseudo Stern–Volmer plot for the ETX fluorescence quenching.[27,33,35,40] The linearity of the corresponding plot was always excellent ($r^2>0.98$) and no deviation was detected at high quencher concentrations. Figure 1 shows a typical example of an exciplex spectrum obtained by the subtraction method for the system ETX/HMB in acetone. Table 1 compiles the quenching rate constants k_Q and the maximum of the exciplex emission bands obtained in several solvents for different aromatic electron donors. It can be seen that all MeB quenchers form exciplexes with ETX in all solvents studied, whereas MeOBs react in a different way: in polar solvents, MeOBs with low oxidation potential did not form emissive exciplexes, contrary to those with high oxidation potential such as anisole. In low polar media, MeOBs with high electron-donor abilities, such as 135MeOB or 12MeOB, also formed weakly emissive exciplexes with ETX. HinMeB did not form any exciplexes with ETX, regardless of the solvent used.

Figure 2 plots log k_Q versus ΔG_{et} in acetonitrile for the entire set of donors. The free-energy change ΔG_{et} for the electron-transfer reaction was calculated by the Rehm–Weller relationship, in which the coulombic interaction was neglected [Eq. (2)].[1]

$$\Delta G_{et} = E_{ox}(D) - E_{red}(ETX) - E_{0,0} \qquad (2)$$

Note that the resulting values of ΔG_{et} are then used in either polar or nonpolar solvents, without any correction.

Discussion

It can be observed from Figure 2 that MeBs exhibit higher reactivity than MeOBs or HinMeBs at the same ΔG_{et} value. In the case of TTB, the rate constant was so low that, within experimental error, no quenching was measured until the quencher solubility limit was reached. It has already been

Table 1. Rate constants k_Q and exciplex maximum emission energies $h\nu_{exc}$ of the fluorescence quenching of ETX by aromatic electron donors in various solvents.

Donor	E_{ox}[b] [V/SCE]	Solvent $(f-1/2f')$[a] ΔG_{et}[c] [eV]	Acetonitrile 0.392 $\log k_Q$	$h\nu_{exc}$	Acetone 0.374 $\log k_Q$	$h\nu_{exc}$	Butyl acetate 0.291 $\log k_Q$	$h\nu_{exc}$	Ethyl acetate 0.293 $\log k_Q$	$h\nu_{exc}$	Dipropyl ether 0.213 $h\nu_{exc}$	CCl_4 0.119 $h\nu_{exc}$
HMB	1.59	−0.04	9.97	2.48	9.8	2.53	9.83	2.62	9.85	2.60	2.69	2.63
durene	1.82	0.19	9.23	2.70	8.99	2.72	9.4	2.74	9.35	2.73	2.79	2.74
124MeB	1.88	0.25	8.61	2.73	8.28	2.75	8.97	2.77	8.88	2.76	2.84	2.80
135MeB	2.07	0.44	8.48	2.74	8.45	2.75	8.96	2.77	8.91	2.76	2.83	2.78
m-xylene	2.14	0.51	8.11	2.78	8.15	2.79	8.72	2.81	8.51	2.80	2.86	2.87
toluene	2.4	0.77	8.05	2.79	8.11	2.83	8.38	2.85	8.42	2.84	2.87	2.88
HEB	1.59	−0.04	8	–	7.9	–	8.1	–	8.22	–	–	–
OMA	1.84	0.21	5.72	–	5.9	–	6.42	–	6.35	–	–	–
TTB	2.1	0.47	nm	–	nm	–	nm	–	nm	–	–	–
1245MeOB	0.81	−0.82	10.33	–	10.36	–	10.05	–	10.09	–	–	–
124MeOB	1.13	−0.5	10.28	–	10.28	–	9.95	–	9.87	–	–	2.19
14MeOB	1.3	−0.33	10.15	–	10.25	–	9.83	–	9.91	–	–	2.50
12MeOB	1.45	−0.18	9.86	–	10.09	2.26	9.65	2.49	9.72	2.48	2.73	2.69
135MeOB	1.49	−0.14	9.78	2.40	9.83	2.48	9.51	2.60	9.42	2.59	2.75	2.72
13MeOB	1.51	−0.12	9.64	2.57	9.25	2.64	9.28	2.75	9.11	2.74	2.8	2.75
anisole	1.75	0.12	7.98	2.75	7.66	2.79	8.87	2.85	8.71	2.84	2.89	2.87
4MeAnisole	1.56	−0.07	9.28	2.62	8.58	2.70	9.24	2.78	9.15	2.77	2.83	2.78

[a] Solvent polarizability-reorientation function, see text. [b] Oxidation potentials of donor taken from reference [41] or measured in the same conditions. [c] Electron-transfer free-energy change calculated by Equation (2). (−) no exciplex emission detected (nm) too low to be properly measured.

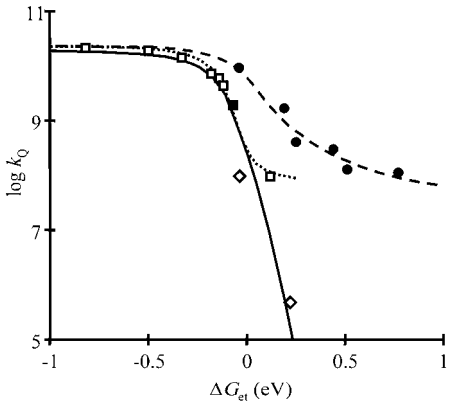

Figure 2. Plots of the logarithm of quenching rate constants k_Q versus charge-transfer free-energy change ΔG_{et} in acetonitrile: (●) MeB, (□) MeOB, (■) 4-methylanisole, (◇) HinMeB. Original Rehm–Weller curve (bold line) and best fits of the experimental data by the exciplex kinetic model for MeB (dashed line) and MeOB (dotted line).

shown that steric crowding maintains reactants at large distances, which strongly diminishes the electronic coupling and consequently constrains the two molecules to react through a full electron transfer .[42–45] HinMeB data points follow the Rehm–Weller curve, plotted as the bold line in Figure 2, showing that they actually behave as pure electron donors. This suggests that the electronic coupling controls the relative efficiency of the PET versus exciplex mechanism.

Solvatochromism of exciplex emission bands: It is possible to determine the dipole moment μ_{exc} of the exciplexes from the solvatochromic study of their maximum emission wavelength [Eq. (3)],[5,27,46–48] where $(f-\frac{1}{2}f')=\left[\frac{\varepsilon-1}{2\varepsilon+1}-\frac{1}{2}\frac{(n^2-1)}{(n^2+1)}\right]$ is the solvent polarizability-reorientation function, ν_{max} is the maximum of the exciplex emission in solution, ν^0_{max} is the hypothetical gas phase exciplex fluorescence maximum and ρ is the Onsager's cavity radius.

$$\nu_{max}=\nu^0_{max}-\frac{2\mu^2_{exc}}{hc\rho^3}(f-\frac{1}{2}f') \quad (3)$$

The plot of ν_{max} versus $(f-\frac{1}{2}f')$ gives a straight line (Figure 3a). As solvatochromic plots are more consistent with a set of solvents having similar refractive indexes, CCl_4 was not used for the determination of exciplex dipole moments.[46] Table 2, which gathers the calculated values of ρ and the corresponding μ_{exc} values obtained from Equation (3), reveals a decrease of μ_{exc} with the decrease of donor ability in the two sets of quenchers, as already observed.[27,49] The decrease is surprisingly marked between HMB and durene, the other MeB quenchers having a dipole moment close to that of durene (5–7 D). A comparison of the μ_{exc} values for 12MeOB, 13MeOB, HMB and anisole illustrates that the dipole moment, and consequently the CT character, changes rapidly from 16 D to 8 D in a small range of ΔG_{et}. The most polar exciplex reported in Table 2, obtained with 12MeOB, has no emission in acetonitrile, which is as expected for an exciplex with a high CT degree.[4,5,27,28] Note that for a pure ion pair, and considering the size of the molecules involved in this study, the dipole moment can be expected to reach 16–18 D.[12,27,28] The evolution from exciplexes with a high degree of CT to low polar exciplexes is sudden and localized near $\Delta G_{et}\approx 0$ eV, as shown in Figure 3b by plotting μ_{exc} versus ΔG_{et}. Interestingly, both MeB and MeOB families lie on the same plot, showing that the exciplex dipole moment determined by solvatochromic plots mainly depends on the redox properties of the acceptor/donor systems. However, the real physical meaning of this

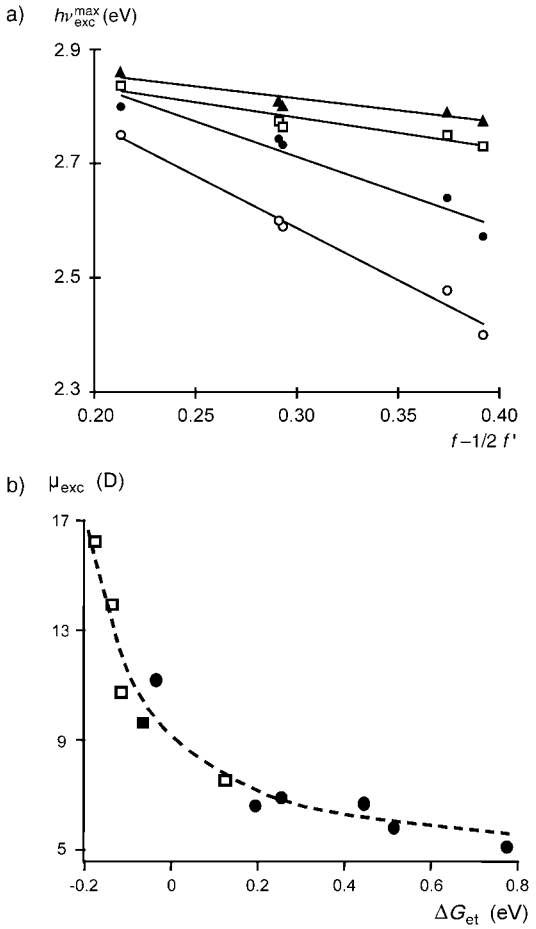

Figure 3. a) Solvatochromic plots (Eq. 3) of the maximum energy of exciplex emission towards the solvent polarizability-reorientation function (f-1/2f'): (▲) m-xylene (□) 124MeB (●) 13MeOB (○) 135MeOB. b) Plot of the exciplex dipole moment vs. free-energy change for the full electron-transfer reaction: (●) MeB, (□) MeOB, (■) 4-methylanisole.

Table 2. Onsager's cavity radii ρ and exciplex dipole moments μ_{ex} for the different electron donors. Dipole moments result from solvatochromic plots [Eq. (4)]. Electron-transfer free-energy change ΔG_{et} extracted from Table 1.

Donor	ρ[Å]	ΔG_{et} [eV]	μ_{ex} [D]
HMB	5.23	−0.04	11.3
durene	5.01	0.19	6.7
124MeB	4.87	0.25	7.0
135MeB	4.89	0.44	6.8
m-xylene	4.71	0.51	5.9
toluene	4.51	0.77	5.2
12MeOB	4.85	−0.18	16.3
135MeOB	5.12	−0.14	14.0
13MeOB	4.90	−0.12	10.8
anisole	4.60	0.12	7.6
4MeAnisole	4.79	−0.07	9.7

collapse of the two quencher families on a single curve remains unclear at the present time.

Influence of ΔG_{et} in low polar solvents: In low polar solvents, the maximum of the exciplex emission band, $h\nu_{exc}^{max}$, is related to the quantity $(E_{ox}(D)-E_{red}(A))$ for exciplexes with strong CT character [Eq. (4a)],[2,5–7] where the term −0.15 eV originates from the empirical correlation obtained by the Weller's group for numerous systems in nonpolar solvents.[5] For exciplexes with low charge-transfer character, Equation (4a) must include a stabilization term U_S due to the resonance interaction between the LE and CT states [Eq. (4b)][2,5–7]

$$h\nu_{exc}^{max}(\text{high CT}) = E_{ox}(D)-E_{red}(A)-0.15(\text{eV}) \quad (4a)$$

$$h\nu_{exc}^{max}(\text{low CT}) = E_{ox}(D)-E_{red}(A)-0.15-U_S(\text{eV}) \quad (4b)$$

The degree of failure of Equation (4a) is interpreted as a measure of the stabilization energy U_S, as shown in Figure 4.

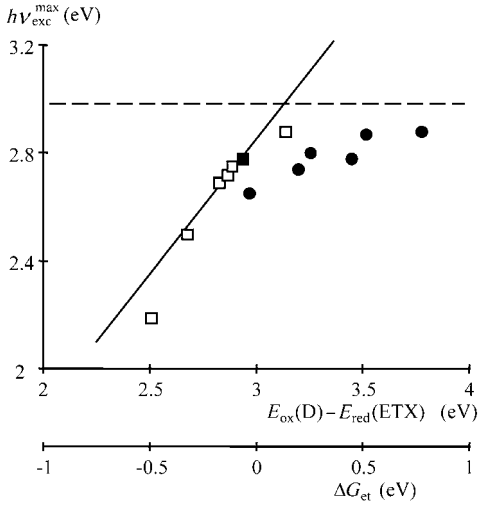

Figure 4. Plots of $h\nu_{exc}^{max}$ versus $(E_{ox}(\text{Donor}-E_{red}(\text{ETX}))$ or ΔG_{et} for (●) MeB (□) MeOB and (■) 4-methylanisole in CCl_4. Bold line: correlation (4a). Dashed line: energy of the first excited singlet state of ETX.

The agreement is good between the MeOB quenchers and Equation (4a). The quencher anisole forms a less polar exciplex than the other MeOB, as can be seen from its lower value of μ_{exc} in Table 2. The LE state is accordingly more involved in the mixing, the stabilization energy U_S being higher than for the other compounds. The fact that most of MeOB follow the correlation given by Equation (4a) is in agreement with the large values of exciplex dipole moments (Table 2). This confirms that most of the MeOB quenchers form polar exciplexes with ETX.

The deviation of the experimental data from Equation (4a) in the endergonic region (Figure 4) implies that U_S becomes important. A valuable comparison can be made between the positions of HMB and 4MeAnisole data. In spite of the higher dipole moment of the HMB exciplex (11.3 D, see Table 2), this is the methoxy-substituted compound which correlates well with Equation (4a). A similar trend is observed between anisole and durene: both have an exciplex dipole moment around 7 D but durene departs more strongly from Equation (4a). This indicates that the stabilization term U_S for MeB exciplexes is higher than for MeOB

and is not related to the polarity feature of the exciplex. The comparison of MeB and HinMeB quenchers in Figure 2 have shown that electronic coupling governs the balance between exciplex and PET mechanisms. In agreement with this result obtained for kinetic data, the difference in terms of stabilization energy is then certainly related to a difference in the value of β, since the value of the resonance integral depends on the ability of electronic coupling between acceptor and donor molecules.[27,28]

Analysis of kinetic data: The diffusional kinetic scheme (Scheme 1) that describes fluorescence quenching was postulated three decades ago,[50] in analogy with the scheme proposed by Rehm and Weller for a full electron-transfer reaction[1] and assuming that k_p accounts for all the deactivation pathways.

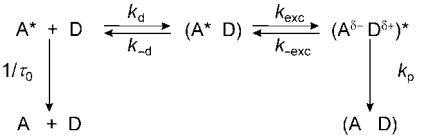

Scheme 1.

Application of the steady-state approximation to Scheme 1 yields Equation (5).

$$k_Q = \frac{k_d}{1+\frac{k_{-d}}{k_{exc}}\left(1+\frac{k_{-exc}}{k_p}\right)} \tag{5}$$

An exciplex model based on this scheme has already been proposed.[17] However, the influence of the solvent was not explicitly taken into account. As k_Q values are determined in solution, the surrounding medium can not be ignored, and it is a real challenge to describe its interaction with reactants. Experimental data have shown that solvent can influence the structure of the exciplex, principally through change of the medium polarity.[2–22] It is especially true in the exergonic region of ΔG_{et}, where exciplexes are quite polar. The role of the surrounding medium on the exciplex structure can be accounted for through a global reorganization energy term λ (Figure 5).[18]

The parabolic model of Marcus[23,24] can be used to relate the potential energy of CT and LE states to the reaction coordinate q [Eq. (6) and (7)], where λ is the sum of the solvent and reactants reorganization energy to go from the LE to the pure CT state.

$$E_{LE} = \lambda q^2 \tag{6}$$

$$E_{CT} = \Delta G_{et} + \lambda(1-q)^2 \tag{7}$$

The reaction coordinate q describes both the nuclear reorganization of the solvent cage and the redistribution of excitation energy over the two reactants. As the formation of

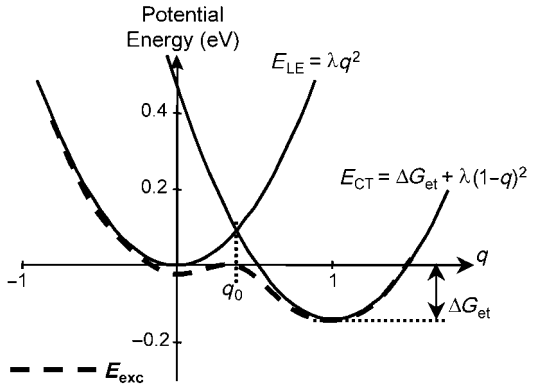

Figure 5. Parabola of potential energy for the locally excited (LE) and the charge-transfer (CT) states. The resulting exciplex energy E_{exc} is indicated by the dashed curve. q_0 is the reaction coordinate corresponding to the crossing point of the two parabola.

exciplexes is a strongly adiabatic reaction, large interaction occurs between the two parabolic curves before the crossing point. This interaction is quantified by the value of the resonance integral $\beta = \langle \Psi_{LE}/\mathscr{H}/\Psi_{CT}\rangle$. The exciplex potential energy E_{exc} remains on the resulting adiabatic curve (see Figure 5). E_{exc} can be calculated from the exciplex wavefunction [Eq. (8)], under the assumption that the spatial integral $S = \langle \Psi_{LE}/\Psi_{CT}\rangle$ can be neglected.

$$E_{exc} = \frac{(E_{LE}+E_{CT})}{2} - \sqrt{\left(\frac{E_{LE}-E_{CT}}{2}\right)^2 + \beta^2} \tag{8}$$

The additional stabilization energy due to the resonance is given by Equation (9).[18]

$$E_{stab} = E_{LE} - E_{exc} \tag{9}$$

ΔG_{exc} can be calculated from the potential energy curves reported in Figure 5 by averaging the corresponding quantity over the whole range of q, which is noted by the symbol $\langle\rangle_q$ (see Appendix). The final relation is given by Equation (10), which relates the microscopic potential energy curves (via E_{stab}) to the macroscopic quantity ΔG_{exc}.

$$\Delta G_{exc} = RT\ln\left[\langle \exp\left(-\frac{E_{stab}(q)}{RT}\right)\rangle_q\right] \tag{10}$$

As E_{stab} depends on ΔG_{et} through Equations (6)–(9), Equation (10) constitutes a relationship between ΔG_{exc} and ΔG_{et}, and therefore is the central equation of the exciplex model. Finally, the Agmon–Levine relationship was used to evaluate $\Delta G_{exc}^{\neq}$ from ΔG_{exc}. This is justified by the fact that the relationship applies in strongly adiabatic charge-transfer process,[54] as was initially shown by Marcus.[55] The parameter $\Delta G_{exc}^{\neq}(0)$ represents the ability of the exciplex to dissipate the reaction energy [Eq. (11)].

$$\Delta G^{\neq}_{exc} = \Delta G_{exc} + \frac{\Delta G^{\neq}_{exc}(0)}{\ln(2)} \ln\left[1 + \exp\left(-\frac{\Delta G_{exc} \times \ln(2)}{\Delta G^{\neq}_{exc}(0)}\right)\right] \quad (11)$$

The rate constants k_{exc} and k_{-exc} are then given by Equations (12) and (13), with $k_0 = 10^{11} s^{-1}$ the collision frequency in solution.[1,17,18] The deactivation rate constant k_p is assumed to be constant on the whole range of ΔG_{et}.

$$k_{exc} = k_0 \times \exp\left(\frac{-\Delta G^{\neq}_{exc}}{RT}\right) \quad (12)$$

$$k_{-exc} = k_{exc} \times \exp\left(\frac{\Delta G_{exc}}{RT}\right) \quad (13)$$

By use of this new model, no assumption was made on either the relative magnitude of k_{-exc} and k_0, or on the reversibility of the exciplex formation, in contrast to reference [18]. Consequently, this model appears to generalize the ones proposed in the literature[17,18] and rationalize the exciplex formation through three main parameters: 1) β, which characterizes the overall interaction of the partners within the exciplex, 2) λ, which describes the exciplex/solvent interaction and 3) k_p, which is related to the lifetime of the exciplex.

The fluorescence quenching rate constants k_Q were fitted by this model using $\Delta G^{\neq}_{exc}(0)$ fixed at 0.12 eV, a typical value in the Agmon–Levine relationship.[56,57] The diffusion rate constant k_d was taken as $3 \times 10^{10} M^{-1} s^{-1}$ in acetonitrile and acetone, and $1.3 \times 10^{10} M^{-1} s^{-1}$ in ethyl acetate, these values being close to the estimations that can be made from the Stokes–Einstein equation.[58] The diffusion equilibrium constant is given by Equation (14).

$$K_d = \frac{k_d}{k_{-d}} \quad (14)$$

The value was fixed at $0.8 M^{-1}$ in the three solvents. λ, β and k_p were taken as adjustable parameters to minimize the sum of square errors χ^2. The results are reported in Table 3.

Table 3. Parameter values resulting from best fits of the experimental data by the exciplex model.

System	λ [eV]	β [eV]	k_p [10^9 s^{-1}]	χ^2
ETX/MeB/MeCN	0.25	0.253	0.011	0.134
ETX/MeOB/MeCN	0.35	0.137	0.026	0.020
ETX/MeB/acetone	0.26	0.20	0.033	0.206
ETX/MeOB/acetone	0.465	0.095	0.026	0.183
ETX/MeB/ethyl acetate	0.25	0.24	0.04	0.109
ETX/MeOB/ethyl acetate	0.42	0.135	0.13	0.415

Figure 2 shows the best fitted curves obtained in acetonitrile. Similar agreement between experimental data and theoretical curves was observed for the fits of MeOB and MeB k_Q values in both acetone and ethyl acetate.

The values of k_p reported in Table 3 are of the same order of magnitude ($\sim 3x10^7 s^{-1}$), except for the system ETX/MeOB in ethyl acetate ($k_p = 1.3x10^8 s^{-1}$); k_p tends to increase as the solvent polarity decreases. More interestingly, the resonance integral β for MeB is about twice the value obtained for MeOB (Table 3). As a consequence, the MeB exciplexes are less sensitive to the effect of the surrounding medium than the MeOB ones, in line with the fact that the λ value for MeB is found to be two times lower than for MeOB. Note that λ is markedly lower than the solvent-reorganization energy generally found for full electron transfer (often more than 1 eV[4]), since the solvent cage must accommodate a weaker dipole-moment change. This quantitatively supports the proposition that the resonance integral β is the key parameter controlling the efficiency of fluorescence quenching by an exciplex mechanism.

Comparison of kinetic with spectroscopic data: The values of λ and β resulting from the fit of kinetic data (k_Q values) by the exciplex model allows the evaluation of ΔG_{exc} through the set of Equations (5)–(13) (Table 4). On the other hand, ΔG_{exc} is related to the energy difference between the maximum emission frequency of ETX and the exciplex, $h\Delta\nu_{fluo} = h(\nu^{max}_{ETX} - \nu^{max}_{exc})$, by Equation (15),[27–29] where U_{FC} is the Franck–Condon relaxation energy of the exciplex. It is therefore tempting to compare $h\Delta\nu_{fluo}$ and ΔG_{exc}, that is, to check the accuracy of the exciplex model for describing both kinetic and spectroscopic results with coherent values of λ and β.

Table 4. Thermodynamic properties of the exciplexes in ethyl acetate.

Compounds	$-\Delta G_{exc}$ [eV][a]	$h\Delta\nu_{fluo}$ [eV][b]
HMB	0.20	0.265
durene	0.12	0.14
124MeB	0.11	0.12
135MeB	0.08	0.11
m-xylene	0.073	0.075
toluene	0.056	0.046
12MeOB	0.20	0.395
135MeOB	0.17	0.29
13MeOB	0.15	0.14
anisole	0.12	0.11
4MeAnisole	0.037	0.046

[a] Calculated from Equations (5)–(13). [b] Evaluated from experimental data $h\Delta\nu_{fluo} = h(\nu^{max}_{ETX} - \nu^{max}_{exc})$ using $\nu^{max}_{ETX} = 2.89$ eV in ethyl acetate.

$$h\Delta\nu_{fluo} = -\Delta G_{exc} + U_{FC} \quad (15)$$

This comparison is given in Figure 6, which clearly proves that the model is perfectly consistent with the two independent sets of experimental data (kinetic and spectroscopic). Indeed, a single linear correlation is found for both MeOB and MeB families of donors [Eq. (16)].

$$-\Delta G_{exc} = 0.89 h\Delta\nu_{fluo} + 0.004 \quad r^2 = 0.85 \quad (16)$$

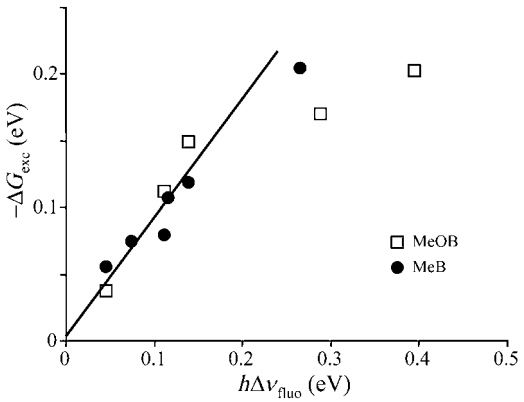

Figure 6. Comparison between kinetic data ($-\Delta G_{exc}$ obtained from kinetic analysis) and spectroscopic data ($h\Delta\nu_{fluo}$) in ethyl acetate. See Table 4.

The three points at the highest $h\Delta\nu_{fluo}$ values, which slightly deviates from Equation (16) were not taken into account in this correlation. The deviation could be ascribed to a decrease of U_{FC} for highly exergonic reactions and rationalized by considering that the exciplex dipole moments are high: $\mu_{exc} > 11$ D for these compounds (Table 2). This behavior was thoroughly analyzed by Kuzmin.[53] However, this does not challenge the important conclusion ensuing from Figure 6: the present exciplex model is definitely supported by the good correlation between ΔG_{exc} (estimated from the fit of kinetic data) and spectroscopic data ($h\Delta\nu_{fluo}$).

Conclusion

ETX fluorescence quenching by methoxybenzenes and methylbenzenes through exciplex formation was studied in a wide variety of solvents, from nonpolar to polar ones. Interestingly, exciplexes were formed in both the endergonic and exergonic regions. Kinetic data were explained on the basis of a new theoretical description, which allowed one to focus on the role of the resonance integral β. It is shown that the donor structure strongly influences the exciplex formation. More importantly, the energetic parameters derived from the fit of kinetic data by the model are in excellent agreement with the spectroscopic data, supporting the validity of this approach.

Appendix

ΔG_{exc} can be calculated from the potential energy surface (Figure 5) [Eq. (A1)].

$$\Delta G_{exc} = \mathrm{RTln}\left[\frac{\int_{-\infty}^{+\infty} \exp\left(-\frac{E_{LE}(q)}{RT}\right)\mathrm{dq}}{\int_{-\infty}^{+\infty} \exp\left(-\frac{E_{exc}(q)}{RT}\right)\mathrm{dq}}\right] \quad \text{(A1)}$$

As $E_{LE}(q) = E_{stab}(q) + E_{exc}(q)$, Equation (A2) can be derived.

$$\Delta G_{exc} = RT\ln\left[\frac{\int_{-\infty}^{+\infty} \exp\left(-\frac{E_{exc}(q)}{RT}\right) \times \exp\left(-\frac{E_{stab}(q)}{RT}\right)\mathrm{dq}}{\int_{-\infty}^{+\infty} \exp\left(-\frac{E_{exc}(q)}{RT}\right)\mathrm{dq}}\right] \quad \text{(A2)}$$

The integrals in the numerator of the fraction in brackets correspond to a thermal averaging of the quantity $\exp\left(-\frac{E_{stab}(q)}{RT}\right)$ over the whole coordinate q, taking into account the Boltzmann distribution of probability to reach a given coordinate q, $\exp\left(-\frac{E_{exc}(q)}{RT}\right)$. The denominator of the fraction is a normalization factor w [Eq. (A3)].

$$w = \int_{-\infty}^{+\infty} \exp\left(-\frac{E_{exc}(q)}{RT}\right)\mathrm{dq} \quad \text{(A3)}$$

As done in reference [18], any quantity $f(q)$ which depends on the reaction coordinate can be thermally averaged by this procedure. It is useful to introduce the notation $\langle f(q)\rangle_q$ used in reference [18] to shorten the writing of integrals [Eq. (A4)].

$$\langle f(q)\rangle_q = \frac{1}{w}\int_{-\infty}^{+\infty} f(q) \times \exp\left(-\frac{E_{exc}(q)}{RT}\right)\mathrm{dq} \quad \text{(A4)}$$

Then Equation (A2) can be rewritten as Equation (A5)

$$\Delta G_{exc} = RT\ln\left[\left\langle \exp\left(-\frac{E_{stab}(q)}{RT}\right)\right\rangle_q\right] \quad \text{(A5)}$$

Acknowledgements

Manuel Dossot is very grateful to Dr. Eric Vauthey for many valuable enthusiastic discussions. Frederic Louerat is also greatly thanked for the synthesis of 1245MeOB. The "Fondation de l'Ecole de Chimie de Mulhouse" is acknowledged for financial support of this work.

[1] D. Rehm, A. Weller, *Isr. J. Chem.* **1970**, *10*, 259.
[2] H. Knibbe, D. Rehm, A. Weller, *Ber. Bunsenges. Phys. Chem.* **1968**, *72*, 257.
[3] N. Mataga, *Pure Appl. Chem.* **1984**, *56*, 1255.
[4] I. G. Gould, S. Farid, *Acc. Chem. Res.* **1996**, *29*, 522.
[5] A. Weller, in *The Exciplex*, (Eds.: M. Gordon, W. R. Ware), Academic Press, New York, 1975, p. 23.
[6] A. Weller, *Z. Phys. Chem. (Muenchen Ger.)* **1982**, *133*, 93.
[7] A. Weller, *Pure Appl. Chem.* **1982**, *54*, 1885.
[8] N. Mataga, H. Miyasaka, *Adv. Chem. Phys.* **1999**, *107*, 431.
[9] N. Mataga, *Pure Appl. Chem.* **1997**, *69*, 729.
[10] K. S. Peters, *Adv. Electron Transfer Chem.* **1994**, *4*, 27.
[11] I. R. Gould, R. H. Young, L. J. Mueller, A. C. Albrecht, S. Farid, *J. Am. Chem. Soc.* **1994**, *116*, 8188.
[12] I. R. Gould, R. H. Young, L. J. Mueller, S. Farid, *J. Am. Chem. Soc.* **1994**, *116*, 8176.

[13] I. R. Gould, D. Noukakis, L. Gomez-Jahn, R. H. Young, J. L. Goodman, S. Farid, *Chem. Phys.* **1993**, *176*, 439.
[14] I. R. Gould, S. Farid, *J. Phys. Chem.* **1992**, *96*, 7635.
[15] I. R. Gould, S. Farid, R. H. Young, *J. Photochem. Photobiol. A* **1992**, *65*, 133.
[16] T. N. Inada, C. S. Miyazawa, K. Kikuchi, M. Yamauchi, T. Nagata, Y. Takahashi, H. Ikeda, T. Miyashi, *J. Am. Chem. Soc.* **1993**, *115*, 7211.
[17] M. G. Kuz′min, *J. Photochem. Photobiol. A* **1996**, *102*, 51.
[18] R. E. Föll, H. E. A. Kramer, U. E. Steiner, *J. Phys. Chem.* **1990**, *94*, 2476.
[19] A. I. Novaira, C. D. Borsarelli, J. J. Costa, C. M. Previtali, *J. Photochem. Photobiol. A* **1998**, *115*, 43.
[20] V. N. Grosso, C. A. Chesta, C. M. Previtali, *J. Photochem. Photobiol. A* **1998**, *118*, 157.
[21] R. Rathore, S. M. Hubig, J. K. Kochi, *J. Am. Chem. Soc.* **1997**, *119*, 11468.
[22] S. M. Hubig, T. M. Bockman, J. K. Kochi, *J. Am. Chem. Soc.* **1996**, *118*, 3842.
[23] R. A. Marcus, N. Sutin, *Biochim. Biophys. Acta* **1985**, *811*, 265.
[24] R. A. Marcus, *J. Chem. Phys.* **1956**, *24*, 966.
[25] F. Brouwer in *Conformational Analysis of Molecules in Excited States*, (Ed.: J. Waluk), Wiley-VCH, New York, **2000**, p. 177.
[26] M. C. Rath, H. Pal, T. Mukherjee, *J. Phys. Chem. A* **2001**, *105*, 7945.
[27] Y. L. Chow, C. I. Johansson, *J. Phys. Chem.* **1995**, *99*, 17558.
[28] Y. L. Chow, C. I. Johansson, *J. Phys. Chem.* **1995**, *99*, 17566.
[29] Y. L. Chow, S.-S. Wang, Z.-L. Liu, V. Wintgens, P. Valat, J. Kossanyi, *New J. Chem.* **1994**, *18*, 923.
[30] K. Kikuchi, *J. Photochem. Photobiol. A* **1992**, *65*, 149.
[31] K. Kikuchi, T. Niwa, Y. Takahashi, H. Ikeda, T. Miyashi, M. Hoshi, *Chem. Phys. Lett.* **1990**, *173*, 421.
[32] C. D. Borsarelli, C. A. Chesta, J. J. Cosa, B. Crystall, D. Phillips, *Chem. Phys. Lett.* **1995**, *232*, 103.
[33] X. Ci, D. G. Whitten, *J. Phys. Chem.* **1991**, *95*, 1988.
[34] M. Dossot, D. Burget, X. Allonas, P. Jacques, *New J. Chem.* **2001**, *25*, 194.
[35] P. Jacques D. Burget, *New J. Chem.* **1995**, *19*, 1061.
[36] A. Zweig, *J. Phys. Chem.* **1963**, *67*, 506.
[37] N. Bodor, Z. Gabanyi, C. Wong, *J. Am. Chem. Soc.* **1989**, *111*, 3783.
[38] A. Gavezotti, *J. Am. Chem. Soc.* **1983**, *105*, 5220.
[39] D. Burget, P. Jacques, *J. Lumin.* **1992**, *23*, 177.
[40] Y. L. Chow, C. I. Johansson, *Chem. Phys. Lett.* **1994**, *231*, 541.
[41] P. Jacques, D. Burget, X. Allonas, *New J. Chem.* **1996**, *20*, 933.
[42] P. Jacques, X. Allonas, P. Suppan, M. Von Raumer, *J. Photochem. Photobiol. A* **1996**, *101*, 183.
[43] S. M. Hubig, R. Rathore, J. K. Kochi, *J. Am. Chem. Soc.* **1999**, *121*, 617.
[44] R. Rathore, S. V. Lindeman, J. K. Kochi, *J. Am. Chem. Soc.* **1997**, *119*, 9393.
[45] G. Jones II, S. Chatterjee, *J. Phys. Chem.* **1988**, *92*, 6862.
[46] P. Suppan, *J. Photochem. Photobiol. A* **1990**, *50*, 293.
[47] G. Cosa, C. A. Chesta, *J. Phys. Chem. A* **1997**, *101*, 4922.
[48] K. Bhattacharyya, M. Chowdhury, *Chem. Rev.* **1993**, *93*, 507.
[49] K. N. Grzeskowiak, S. E. Ankner-Mylon, S. N. Smirnov, C. L. Braun, *Chem. Phys. Lett.* **1996**, *257*, 89.
[50] W. R. Ware, *Pure Appl. Chem.* **1975**, *41*, 635.
[51] M. G. Kuz′min, *Russ. J. Phys. Chem.* **1999**, *73*, 1625.
[52] I. V. Soboleva, M. G. Kuz′min, E. V. Dolotova, *High Energy Chem.* **2002**, *36*, 29.
[53] D. N. Dogadkin, I. V. Soboleva, M. G. Kuz′min, *High Energy Chem.* **2002**, *36*, 383.
[54] N. Agmon, R. D. Levine, *Chem. Phys. Lett.* **1977**, *52*, 197.
[55] R. A. Marcus, *J. Chem. Phys.* **1956**, *24*, 966.
[56] G. L. Hug, B. Marciniak, *J. Phys. Chem.* **1995**, *99*, 1478.
[57] F. Scandola, V. Balzani, G. B. Schuster, *J. Am. Chem. Soc.* **1981**, *103*, 2519.
[58] S. L. Murov, I. Carmichael, G. L. Hug, *Handbook of Photochemistry*, 2nd ed., Marcel Dekker Inc., New York, **1993**.

Received: March 19, 2004
Revised: October 27, 2004
Published online: January 25, 2005